



Novel thermal-stable low temperature sintered $\text{Ba}_2\text{LiMg}_2\text{V}_3\text{O}_{12}$ microwave dielectric ceramics with $\text{ZnO-P}_2\text{O}_5\text{-MnO}_2$ glass addition

Cheng Liu*, Huaiwu Zhang, Gang Wang, Tingchuan Zhou, Hua Su, Lijun Jia, Lichuan Jin, Jie Li, Yulong Liao

State Key Laboratory of Electronic Thin Films and Integrated Devices, University of Electronic Science and Technology of China, Chengdu 610054, China

ARTICLE INFO

Article history:

Received 19 December 2016

Received in revised form 28 March 2017

Accepted 22 April 2017

Available online 23 April 2017

Keywords:

Ceramics

Microwave dielectric property

Sintering

Microstructure

ABSTRACT

Novel $\text{Ba}_2\text{LiMg}_2\text{V}_3\text{O}_{12}$ ceramics with different amount of $\text{ZnO-P}_2\text{O}_5\text{-MnO}_2$ (ZPM) glass addition were densified at 850°C via a solid-state reaction route. No reaction between the ceramic matrix and Ag was detected. A $\text{Ba}_3(\text{VO}_4)_2$ secondary phase generated in the $\text{Ba}_2\text{LiMg}_2\text{V}_3\text{O}_{12}$ matrix made a positive contribution to the τ_f value. Further addition of the ZPM glass adjusted the τ_f value to near zero. Among all specimens, the sample with 2 wt.% of the ZPM addition (marked as BZ20) possessed good microwave dielectric properties: $\epsilon_r = 13.47$, $Q \times f = 16272 \text{ GHz}$ (11.18 GHz), $\tau_f = (+)0.4 \text{ ppm}/^\circ\text{C}$. All experimental results suggested that a novel thermal-stable microwave dielectric ceramic system was designed for LTCC applications.

© 2017 Published by Elsevier Ltd.

1. Introduction

Rapid development of wireless communication demands vast amount of microwave components. For most microwave devices, dielectric ceramic materials are widely adopted due to their advantages in compactness, thermal stability, light weight, and low cost for high frequency applications [1]. Further development of device miniaturization and integration requires that the ceramic could be cofired with the internal metal electrodes. Low-temperature co-fired ceramic (LTCC) technology is a superior solution for miniaturization and integration [2]. Silver (Ag), due to its high conductivity and low cost, has been widely used as the internal electrodes, but its melting temperature is only about 961°C [3]. Thus it is essential to explore new low-temperature sintered ceramic systems with good compatibility between the dielectric matrix and silver electrodes [4,5].

For most microwave devices, the frequency determining components require that the dielectric materials should possess moderate permittivity (ϵ_r), low dielectric loss (high Q), and nearly zero temperature coefficient of resonant frequency (τ_f) with low cost [1]. However, it is always a challenge to balance and realize these performance indexes within one single material. Therefore, various material systems with different crystal structure were

investigated to break the limitations [6–9]. Among these materials, garnet-type compounds were reported as promising candidates in the field of lasers, phosphors, and ferrite materials [10–12], whereas few results were related with their microwave dielectric properties. Recently, the microwave dielectric properties of the $\text{Re}_3\text{Ga}_5\text{O}_{12}$ ($\text{Re} = \text{Nd, Sm, Eu, Dy, Yb, and Y}$) garnets were uncovered and promising microwave dielectric performance were obtained: high $Q \times f$ ($>40000 \text{ GHz}$), low ϵ_r value (~ 12), and relatively stable τ_f values (-33.7 to $-12.4 \text{ ppm}/^\circ\text{C}$) [13]. However, their sintering temperatures are usually too high (1350°C – 1500°C) to apply for LTCC technology. Fortunately, some modified garnet vanadates were reported with low sintering temperatures and good microwave dielectric properties, which are potential for LTCC applications [14–16]. Fang et al. reported that the $\text{LiCa}_3\text{MgV}_3\text{O}_{12}$ ceramic sintered at 900°C showed a low ϵ_r value of 10.5, a high $Q \times f$ value of 74700 GHz , and a τ_f value of $-61 \text{ ppm}/^\circ\text{C}$ [14]. Further exploration on $\text{NaCa}_2\text{Mg}_2\text{V}_3\text{O}_{12}$ ceramics reached to a similar result: a low ϵ_r value of 10, a relative high $Q \times f$ value of 50600 GHz , and a τ_f value of $-47 \text{ ppm}/^\circ\text{C}$ when sintered at 915°C [15]. These results indicated that the modified garnet vanadates possess relatively high $Q \times f$ values when sintered at low temperature, but their large negative τ_f values prohibited their practical applications. Therefore, it is essential to search for new garnet microwave dielectric systems with a near-zero temperature coefficient of resonant frequency.

As known, phosphate glass is promising for its eco-friendly compatibility with low-melting-point below 600°C , which is

* Corresponding author.

E-mail address: c_liu@uestc.edu.cn (C. Liu).

beneficial for LTCC technology [17–19]. But the P_2O_5 based phosphate glass usually possesses relatively poor chemical stability, thus different oxides such as ZnO, MnO_2 , Al_2O_3 , and CuO have been adopted to improve its performance [20–22]. Among these modified systems, ZnO- P_2O_5 - MnO_2 based system is promising due to its lower ternary eutectic temperature and better performance in low temperature, which is widely applied in electronic packaging area. Based on these promising characteristics, ZnO- P_2O_5 - MnO_2 glass might be a suitable sintering aid for garnet-structured microwave dielectrics.

In this study, novel $Ba_2LiMg_2V_3O_{12}$ ceramic system with different amount of ZnO- P_2O_5 - MnO_2 (ZPM) glass addition were fabricated via a solid-state reaction route. The microstructure and microwave dielectric properties were investigated systematically. It was revealed that the combined $Ba_3(VO_4)_2$ secondary phase generated in the $Ba_2LiMg_2V_3O_{12}$ matrix with the ZPM glass addition made a positive contribution on τ_f , adjusting its value to near zero, which was promising for microwave applications.

2. Experimental procedure

$Ba_2LiMg_2V_3O_{12}$ powders were synthesized with reagent grade $BaCO_3$, Li_2CO_3 , MgO, and V_2O_5 (all purity > 99%, Sinopharm Chemical Reagent Co. Ltd, Shanghai, China). The starting materials were accurately weighed in stoichiometric ratios, mixed with zirconia media and ethanol by ball milling for 24 h. After drying, the mixture were calcined at 800 °C for 4 h to form the $Ba_2LiMg_2V_3O_{12}$ phase. To ensure the sintering temperature of the $Ba_2LiMg_2V_3O_{12}$ ceramics stay lower, ZnO- P_2O_5 - MnO_2 (ZPM) glass addition was added. The ZPM powders were synthesized with a composition of 65 mol% of ZnO, 30 mol% of P_2O_5 , and 5 mol% of MnO_2 , using reagent grade ZnO, P_2O_5 , and MnO_2 (all purity > 99%, Sinopharm Chemical Reagent Co. Ltd, Shanghai, China). The ZPM mixture was melted at 1100 °C for 30 min in a platinum crucible and followed by a quenching process in cold deionized water to form amorphous ZPM glass. Then the quenched glass was dried and crushed into powders, milled again for 10 h. Then different amount of the ZPM powders ($x = 0$ wt.%, 0.5 wt.%, 1 wt.%, and 2 wt.%) were added into the $Ba_2LiMg_2V_3O_{12}$ matrix. For convenience, we abbreviated these samples as BZx: BZ (0 wt.%), BZ05 (0.5 wt.%), BZ10 (1 wt.%), and BZ20 (2 wt.%), respectively. After re-milling for another 10 h, the dried BZx powders were subsequently granulated with PVA binder and pressed into cylinder-shaped bulks with 12 mm in diameter and 6 mm in thickness. The green bulks were sintered in a temperature range of 800–900 °C for 4 h in air atmosphere.

The bulk densities of the as-sintered samples were measured by Archimedes method. The phase structure of the as-sintered samples were examined by an X-ray diffractometer (XRD: Philips X' pert Pro MPD, PANalytical Company, Almelo, Holland) at a scanning rate of 10°/min in the range of $10^\circ \leq 2\theta \leq 80^\circ$, using $CuK\alpha$ radiation. The microstructure of the as-sintered ceramics was observed using a scanning electron microscope (SEM: JEOL JSM-6490, Tokyo, Japan). The dielectric properties at microwave frequencies were measured by the Hakki-Coleman dielectric resonator method in TE011 mode by using a network analyzer (Agilent N5230A, 300 MHz–20 GHz, Agilent Technologies, Palo Alto, CA, USA) combined with a temperature chamber (Delta 9023, Delta Design, USA). The temperature coefficient of resonant frequency value (TCF, τ_f) can be determined via the following equation [23]:

$$\tau_f = \frac{f_T - f_{T_0}}{f_{T_0} \times (T - T_0)} \times 10^6 \text{ ppm/}^\circ\text{C}$$

where f_T and f_{T_0} were the resonant frequencies at temperature T (85 °C) and T_0 (25 °C), respectively.

3. Results and discussions

Fig. 1 shows the bulk density of the ZPM modified $Ba_2LiMg_2V_3O_{12}$ ceramics at different sintering temperatures. It is observed that the bulk density values for all specimens increase with the sintering temperature, approaching to a maximum value around 850 °C, then decline. It should be pointed out that the densification temperature is slightly shifted towards lower temperatures while the bulk density is increased with introducing the ZPM glass, as the arrow marked in Fig. 1. This sintering behavior demonstrates that pure $Ba_2LiMg_2V_3O_{12}$ ceramics can be fired below 950 °C without any sintering aids, which meets the basic requirements of the LTCC technology; the addition of the ZPM glass can lower the sintering temperature and assist to densify the $Ba_2LiMg_2V_3O_{12}$ ceramics. Based on the above sintering behavior, we select the specimens fired at 850 °C for further investigation.

Fig. 2 shows the XRD patterns of the ZPM modified $Ba_2LiMg_2V_3O_{12}$ ceramics sintered at 850 °C for 4 h. Besides the cubic garnet structured $Ba_2LiMg_2V_3O_{12}$ phase with a lattice parameter of $a = 12.5408 \text{ \AA}$, as indexed with rhombus shape in red, a secondary phase of $Ba_3(VO_4)_2$ with hexagonal crystal structure (R-3m, PDF# 29-0211) is detected (marked with heart shape). As $Ba_3(VO_4)_2$ is also a promising microwave dielectric system with positive τ_f values and high $Q \times f$ values [24,25], this secondary phase may not deteriorate the dielectric performance of this $Ba_2LiMg_2V_3O_{12}$ system. No third phase related with the ZPM glass can be detected.

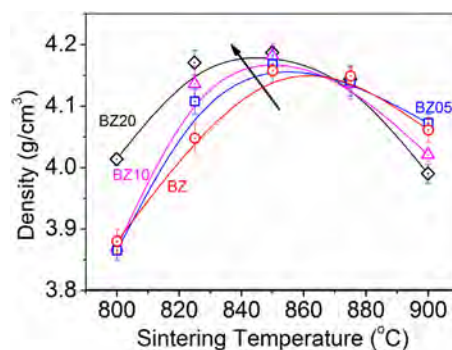


Fig. 1. Bulk density of the ZPM modified $Ba_2LiMg_2V_3O_{12}$ ceramics at different sintering temperatures.

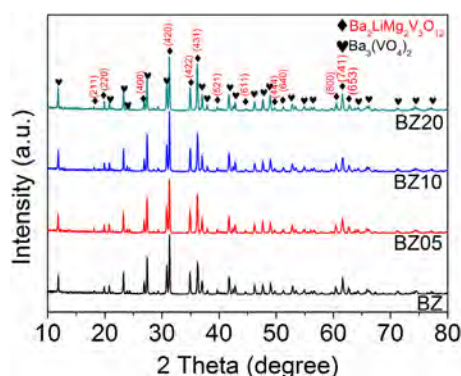


Fig. 2. XRD patterns of the ZPM modified $Ba_2LiMg_2V_3O_{12}$ ceramics sintered at 850 °C for 4 h.

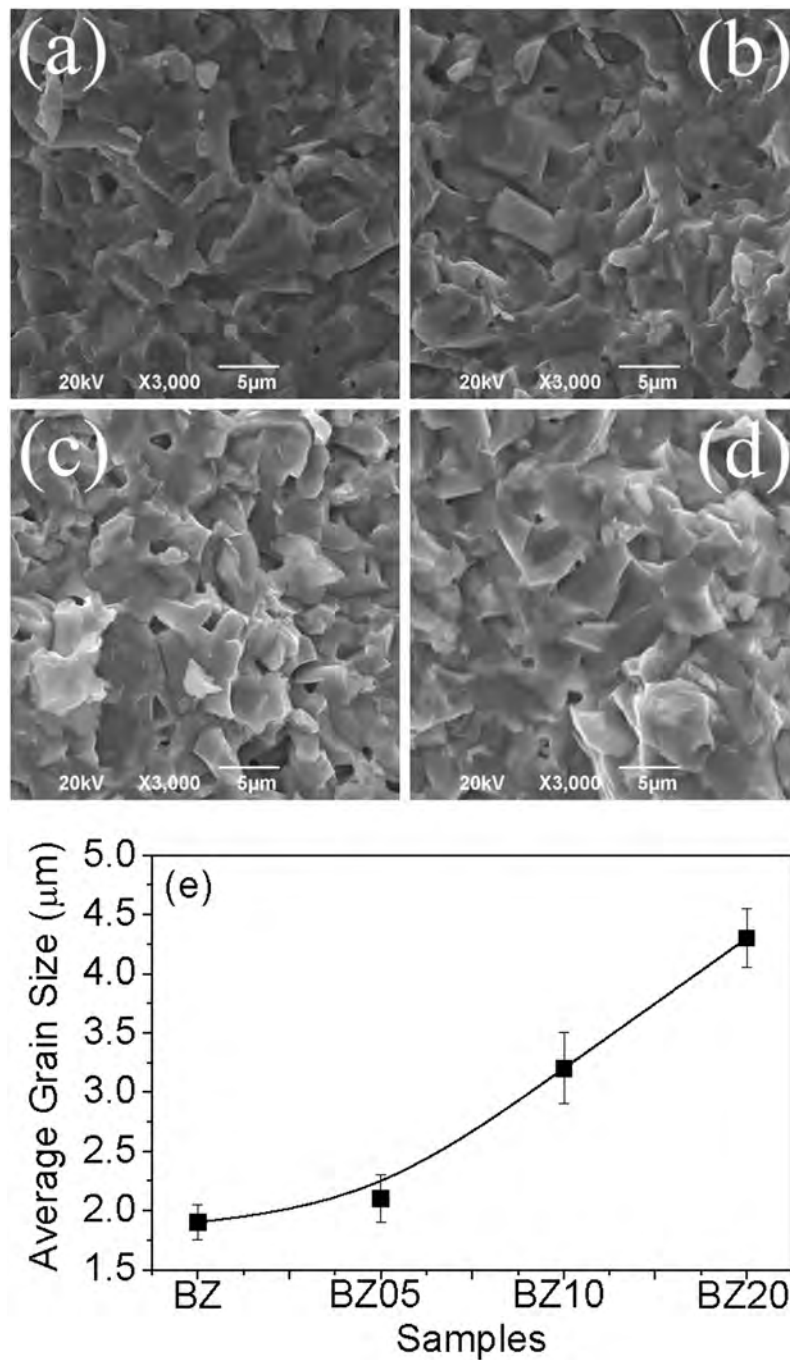


Fig. 3. (a–d) SEM images and (e) variation of the average grain size of the ZPM modified Ba₂LiMg₂V₃O₁₂ ceramics sintered at 850 °C for 4 h.

Fig. 3(a–d) exhibits the SEM images of the ZPM modified Ba₂LiMg₂V₃O₁₂ ceramics sintered at 850 °C for 4 h. Dense morphology with well-stacked grains are observed, but the grain size varies slightly with the ZPM doping amount. Fig. 3(e) shows the variation of the corresponding average grain size calculated from Fig. 3(a–d). It can be observed that the average grain size slightly increases with the ZPM doping level. The average grain size for the pure Ba₂LiMg₂V₃O₁₂ ceramic (BZ) is around 1.9 μm (Fig. 3a); then it increases with introducing the ZPM glass. For the 0.5 wt.% of ZPM doped Ba₂LiMg₂V₃O₁₂ ceramic (BZ05), the average grain size is around 2.1 μm (Fig. 3b); then it inclines up to 3.2 μm for the 1 wt.% of ZPM doped Ba₂LiMg₂V₃O₁₂ ceramic (BZ10) (Fig. 3c); with further increasing the ZPM doping amount to 2 wt.%, the average

grain size of the BZ20 sample is around 4.3 μm (Fig. 3d). These experimental results suggest that the introduction of the ZPM glass can assist the grain growth of the Ba₂LiMg₂V₃O₁₂ ceramics. As known, the liquid phase on grain boundaries could contribute to low activation energy and packed grain construction, which is usually beneficial for the improved microwave dielectric performance [26,27].

Fig. 4 shows the dielectric properties of the ZPM modified Ba₂LiMg₂V₃O₁₂ ceramics sintered at 850 °C for 4 h at microwave frequency. In Fig. 4(a), the dielectric permittivity of the ZPM modified Ba₂LiMg₂V₃O₁₂ ceramics declines with increasing the ZPM doping amount. Generally, the dielectric permittivity should increase with the density. In this study, the density of the ceramics

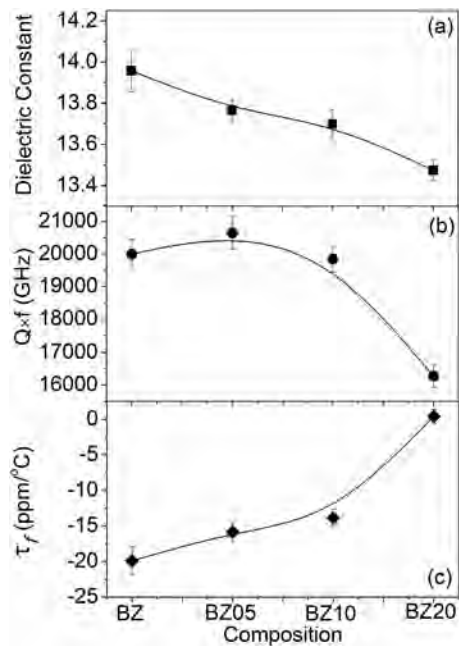


Fig. 4. Microwave dielectric properties of the ZPM modified $\text{Ba}_2\text{LiMg}_2\text{V}_3\text{O}_{12}$ ceramics sintered at 850°C for 4 h.

is increased as well as the amount of the ZPM glass, while the dielectric permittivity of the lead-free ZPM glass is below 10, lower than that of the BM matrix. Therefore, the dielectric constant is an integrated value originated from both the “increase” contribution of densification and the “decrease” contribution of ZPM glass, and it turns out that the latter one dominates. Fig. 4(b) exhibits the variation of the $Q \times f$ value with the ZPM doping amount, which increases slightly from 19994 GHz for BZ to 20645 GHz for BZ05, indicating that a small amount of ZPM addition can assist to enhance the $Q \times f$ value of the $\text{Ba}_2\text{LiMg}_2\text{V}_3\text{O}_{12}$ ceramics; however, the $Q \times f$ value declines with further increasing the ZPM level, reducing to 19842 GHz and 16272 GHz, for BZ10 and BZ20, respectively. Fig. 4(c) exhibits the variation of the τ_f values of the ZPM modified $\text{Ba}_2\text{LiMg}_2\text{V}_3\text{O}_{12}$ ceramics. The τ_f value for BZ is $-19.9 \text{ ppm}/^\circ\text{C}$; then it increases to $-15.8 \text{ ppm}/^\circ\text{C}$ for BZ05 and $-13.9 \text{ ppm}/^\circ\text{C}$ for BZ10, respectively. With the ZPM doping amount increasing up to 2 wt.%, the τ_f value reaches up to $+0.4 \text{ ppm}/^\circ\text{C}$ for

BZ20, indicating that the τ_f value of the $\text{Ba}_2\text{LiMg}_2\text{V}_3\text{O}_{12}$ ceramic system can be adjusted to near zero via adopting suitable amount of ZPM glass addition.

Fig. 5 exhibits a concise schematic diagram of the τ_f evolution of the ZPM modified $\text{Ba}_2\text{LiMg}_2\text{V}_3\text{O}_{12}$ with the $\text{Ba}_3(\text{VO}_4)_2$ secondary phase. As the garnet vanadates usually show high negative τ_f values [14–16], the emergence of the $\text{Ba}_3(\text{VO}_4)_2$ secondary phase, which possesses positive τ_f values [24,25], could contribute to a lowered negative τ_f value due to the offset effect. Thus the absolute τ_f value for BZ is lower than the values of the reported garnet vanadates. Furthermore, the introduction of the ZPM glass plays an important effort on shifting the τ_f value to zero, which is discovered for the first time.

The chemical compatibility of the ceramic matrix with the silver electrode is an essential evaluation indicator for practical applications. Here we study the reactivity of the $\text{Ba}_2\text{LiMg}_2\text{V}_3\text{O}_{12}$ ceramic matrix with Ag powders to evaluate its potential as LTCC materials. Fig. 6 presents the fracture SEM images of the $\text{Ba}_2\text{LiMg}_2\text{V}_3\text{O}_{12}$ ceramics after co-firing with 20 wt% Ag powders at 850°C for 4 h. The Ag part is marked with the red frame in Fig. 6(A), where the EDS analysis on spot A reveals that only Ag element can be detected and no additional elementary peaks are observed. The ceramic area is also marked with the red frame in Fig. 6(B), where the EDS analysis on spot B only reflects the elementary peaks of the $\text{Ba}_2\text{LiMg}_2\text{V}_3\text{O}_{12}$ phase. Meanwhile, a clear boundary between the ceramic matrix and Ag is observed, as marked with the yellow frame in Fig. 6(A, B), suggesting a good contact between each other. Both the SEM and EDS analysis indicate that the $\text{Ba}_2\text{LiMg}_2\text{V}_3\text{O}_{12}$ ceramic matrix does not react with Ag at the sintering temperature. All the above experimental results demonstrate that the ZPM modified $\text{Ba}_2\text{LiMg}_2\text{V}_3\text{O}_{12}$ ceramic system is a suitable candidate for LTCC applications.

4. Conclusions

In this study, $\text{ZnO-P}_2\text{O}_5\text{-MnO}_2$ (ZPM) glass modified $\text{Ba}_2\text{LiMg}_2\text{V}_3\text{O}_{12}$ ceramics were obtained at 850°C via a solid-state reaction route with no reaction between the ceramic matrix and Ag, conforming the requirements of the LTCC applications. The $\text{Ba}_2\text{LiMg}_2\text{V}_3\text{O}_{12}$ main phase with a $\text{Ba}_3(\text{VO}_4)_2$ secondary phase coexisted well and dense crystal morphology were obtained. It is interesting that the τ_f value can be adjusted to near zero via the generation of the $\text{Ba}_3(\text{VO}_4)_2$ secondary phase combined with suitable amount of the ZPM glass addition. Particularly, the sample with 2 wt.% of the ZPM addition (marked as BZ20) possessed good microwave dielectric properties: $\epsilon_r = 13.47$, $Q \times f = 16272 \text{ GHz}$ (11.18 GHz), $\tau_f = (+)0.4 \text{ ppm}/^\circ\text{C}$. Our study suggested that this novel low-temperature sintered garnet vanadate system is a suitable candidate for microwave applications.

Acknowledgements

This work was supported by the National Natural Science Foundation of China (Grant Nos. 51402041, 51672036, and 51602036), the Scientific Research Launch Foundation of UESTC (Grant No. ZYGX2016KYQD092), the National High-Tech Research and Development Program of China (Grant No. 2015AA034102), the National Key Research and Development Plan (Grant No. 2016YFA0300801), and the Science and Technology Department of Sichuan Province (Grant No. 2014GZ0015). This work is also supported in part by the 111 Project (Grant No. B13042), the Fundamental Research Funds for the Central Universities, and the International Science and Technology Cooperation Program of China (Grant No. 2012DFR10730).

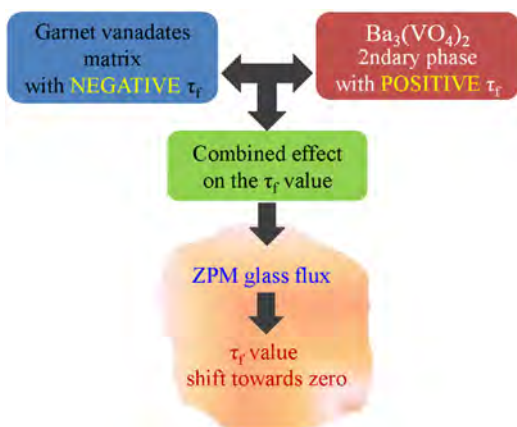


Fig. 5. Schematic diagram of the dielectric property evolution of the $\text{Ba}_2\text{LiMg}_2\text{V}_3\text{O}_{12}$ ceramics with ZPM glass additives.

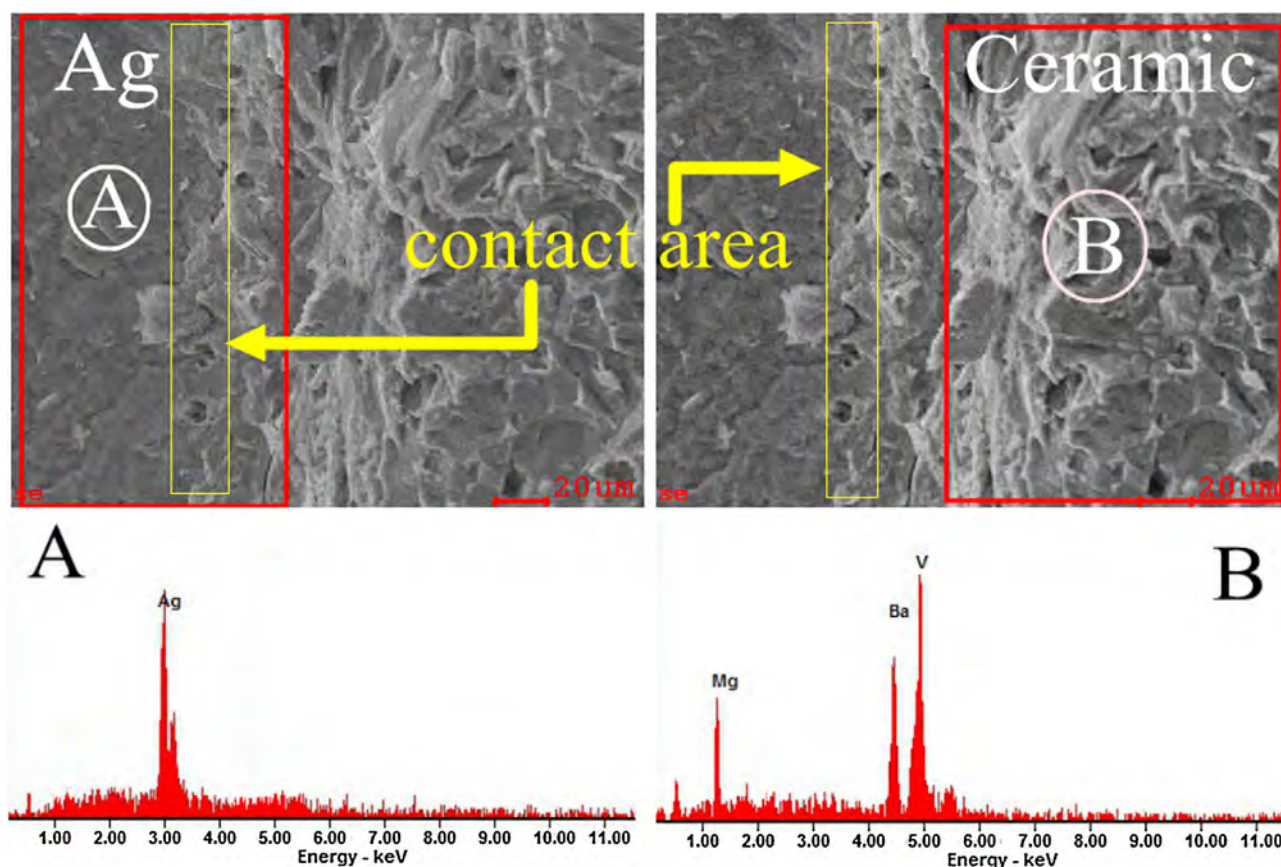


Fig. 6. SEM and EDS analysis of the $\text{Ba}_2\text{LiMg}_2\text{V}_3\text{O}_{12}$ ceramics cofired with Ag at 850 °C for 4 h.

References

- [1] M.T. Sebastian, Dielectric Materials for Wireless Communications, Elsevier Publishers, Oxford, 2008.
- [2] I.M. Reaney, D. Idles, Microwave dielectric ceramics for resonators and filters in mobile phone networks, *J. Am. Ceram. Soc.* 89 (2006) 2063–2072.
- [3] M. Guo, S.P. Gong, G. Dou, D. Zhou, A new temperature stable microwave dielectric ceramics: $\text{znTiNb}_2\text{O}_8$ sintered at low temperatures, *J. Alloys Compd.* 509 (2011) 5988–5995.
- [4] H.F. Zhou, H. Wang, K.C. Li, X. Yao, Microwave dielectric properties of the 5. $7\text{Li}_2\text{O}-\text{Nb}_2\text{O}_5-7.3\text{TiO}_2$ ceramics, *J. Mater. Sci.* 43 (10) (2008) 3725–3727.
- [5] G.G. Yao, P. Liu, H.W. Zhang, Novel series of low-firing microwave dielectric ceramics: $\text{Ca}_5\text{A}_4(\text{VO}_4)_6$ ($\text{A}^{2+} = \text{Mg}, \text{Zn}$), *J. Am. Ceram. Soc.* 96 (6) (2013) 1691–1693.
- [6] J. Zhang, R. Zuo, Effect of ordering on the microwave dielectric properties of spinel-structured $(\text{Zn}_{1-x}(\text{Li}_{2/3}\text{Ti}_{1/3})_x)_2\text{TiO}_4$ ceramics, *J. Am. Ceram. Soc.* 99 (10) (2016) 3343–3349.
- [7] F. Gu, G. Chen, C. Yuan, C. Zhou, T. Yang, Y. Yang, Low temperature sintering and microwave dielectric properties of $0.2\text{Ca}_{0.8}\text{Sr}_{0.2}\text{TiO}_3-0.8\text{Li}_{0.5}\text{Sm}_{0.5}\text{TiO}_3$ ceramics with $\text{BaCu}(\text{B}_2\text{O}_5)$ additive and TiO_2 dopant, *Mater. Res. Bull.* 61 (2014) 245–251.
- [8] C.L. Huang, Y.H. Chien, C.F. Shih, H.Y. Chang, Crystal structure and dielectric properties of $x\text{Ca}(\text{Mg}_{1/3}\text{Nb}_{2/3})\text{O}_3-(1-x)(\text{Ca}_{0.61}\text{Nd}_{0.26})\text{TiO}_3$ at the microwave frequency, *Mater. Res. Bull.* 63 (2015) 1–5.
- [9] C. Hu, P. Liu, Microwave dielectric properties of SiO_2 ceramics with addition of Li_2TiO_3 , *Mater. Res. Bull.* 65 (2015) 132–136.
- [10] J.F. Li, K.H. Qiu, J.F. Li, W. Li, Q. Yang, J.H. Li, A novel broadband emission phosphor $\text{Ca}_2\text{KMg}_2\text{V}_3\text{O}_{12}$ for white light emitting diodes, *Mater. Res. Bull.* 45 (2010) 598–602.
- [11] A. Brenier, Y. Guyot, H. Canibano, G. Boulon, Growth, spectroscopic, and laser properties of Yb^{3+} -doped $\text{Lu}_3\text{Al}_5\text{O}_{12}$ garnet crystal, *J. Opt. Soc. Am. B* 23 (4) (2006) 676–683.
- [12] M. Sugimoto, The past, present, and future of ferrites, *J. Am. Ceram. Soc.* 82 (2) (1999) 269–280.
- [13] J.C. Kim, M.H. Kim, J.B. Lim, S. Nahm, Synthesis of $\text{BaCu}(\text{B}_2\text{O}_5)$ ceramics and their effect on the sintering temperature and microwave dielectric properties of $\text{Ba}(\text{Zn}_{1/3}\text{Nb}_{2/3})\text{O}_3$ ceramics, *J. Am. Ceram. Soc.* 90 (2) (2007) 641–644.
- [14] L. Fang, C.X. Su, H.F. Zhou, Z.H. Wei, H. Zhang, Novel low-firing microwave dielectric ceramic $\text{LiCa}_3\text{MgV}_3\text{O}_{12}$ with low dielectric loss, *J. Am. Ceram. Soc.* 96 (3) (2013) 688–690.
- [15] L. Fang, F. Xiang, C.X. Su, H. Zhang, Novel low firing microwave dielectric ceramic $\text{NaCa}_2\text{Mg}_2\text{V}_3\text{O}_{12}$, *Ceram. Int.* 39 (8) (2013) 9779–9783.
- [16] H.F. Zhou, F. He, X. Chen, J. Chen, L. Fang, W. Wang, Y. Miao, A novel thermally stable low-firing $\text{LiMg}_4\text{V}_3\text{O}_{12}$ ceramic: sintering characteristic, crystal structure and microwave dielectric properties, *Ceram. Int.* 40 (2014) 6335–6338.
- [17] R.K. Brow, D.R. Tallant, Structural design of sealing glasses, *J. Non-Cryst. Solids* 222 (1997) 396–406.
- [18] R. Morena, Phosphate glasses as alternatives to Pb-based sealing frits, *J. Non-Cryst. Solids* 263–264 (2000) 382–387.
- [19] J. Hong, D. Zhao, J. Gao, M. He, H. Li, G. He, Lead-free low-melting point sealing glass in $\text{SnO}-\text{CaO}-\text{P}_2\text{O}_5$ system, *J. Non-Cryst. Solids* 356 (2010) 1400–1403.
- [20] B. Zhang, Q. Chen, D. Wang, Effect of MnO/MnO_2 addition on the properties of low-melting phosphate glasses, *J. Chin. Ceram. Soc.* 36 (4) (2008) 535–538.
- [21] A. Moguš-Milanković, A. Gajović, A. Šantić, D.E. Day, Structure of sodium glasses containing Al_2O_3 and/or Fe_2O_3 , part I, *J. Non-Cryst. Solids* 289 (2001) 204–213.
- [22] P.A. Bingham, R.J. Hand, O.M. Hannant, S.D. Forder, S.H. Kilcoyne, Effects of modifier additions on the thermal properties chemical durability, oxidation state and structure of iron-phosphate glasses, *J. Non-Cryst. Solids* 355 (2009) 1526–1538.
- [23] C. Liu, H.W. Zhang, H. Su, T.C. Zhou, J. Li, X. Chen, W.Z. Miao, L. Xie, L.J. Jia, Low temperature sintering BBSZ glass modified $\text{Li}_2\text{MgTi}_3\text{O}_8$ microwave dielectric ceramics, *J. Alloys Compd.* 646 (2015) 1139–1142.
- [24] S.Q. Meng, Z.X. Yue, H. Zhuang, F. Zhao, L.T. Li, Microwave dielectric properties of $\text{Ba}_3(\text{VO}_4)_2-\text{Mg}_2\text{SiO}_4$ composite ceramics, *J. Am. Ceram. Soc.* 93 (2) (2010) 359–361.
- [25] Y. Lv, R. Zuo, Z. Yue, Structure and microwave dielectric properties of $\text{Ba}_3(\text{VO}_4)_2-\text{Zn}_{2-x}\text{SiO}_{4-x}$ ceramic composites, *Mater. Res. Bull.* 48 (2013) 2011–2017.
- [26] T.C. Zhou, H.W. Zhang, L.J. Jia, Y.L. Liao, Z.Y. Zhong, F.M. Bai, H. Su, J. Li, L.C. Jin, C. Liu, Enhanced ferromagnetic properties of low temperature sintering LiZnTi ferrites with $\text{Li}_2\text{O}-\text{B}_2\text{O}_3-\text{SiO}_2-\text{CaO}-\text{Al}_2\text{O}_3$ glass addition, *J. Alloys Compd.* 620 (2015) 421–426.
- [27] S.R. Kiran, G. Sreenivasulu, V.R.K. Murthy, V. Subramanian, B.S. Murty, Effect of grain size on the microwave dielectric characteristics of high-energy ball-milled zinc magnesium titanate ceramics, *J. Am. Ceram. Soc.* 95 (6) (2012) 1973–1979.